

# Constraint likelihood analysis for a network of gravitational wave detectors

S. Klimenko, S. Mohanty<sup>†</sup>, M. Rakhmanov and G. Mitselmakher  
*University of Florida, P.O.Box 118440, Gainesville, Florida, 32611, USA and*

<sup>†</sup>*The University of Texas at Brownsville, 80 Fort Brown, Brownsville, Texas, 78520, USA*

We propose a coherent method for the detection and reconstruction of gravitational wave signals with a network of interferometric detectors. The method is derived using the likelihood functional for unknown signal waveforms. In the standard approach, the global maximum of the likelihood over the space of waveforms is used as the detection statistic. We identify a problem with this approach. In the case of an aligned pair of detectors, the detection statistic depends on the cross-correlation between the detectors as expected, but this dependence disappears even for infinitesimally small misalignments. We solve the problem by applying constraints on the likelihood functional and obtain a new class of statistics. The resulting method can be applied to data from a network consisting of any number of detectors with arbitrary detector orientations. The method allows us reconstruction of the source coordinates and the waveforms of two polarization components of a gravitational wave. We study the performance of the method with numerical simulation and find the reconstruction of the source coordinates to be more accurate than in the standard approach.

PACS: 04.80.Nn, 07.05.Kf, 95.55.Ym

## I. INTRODUCTION

Several gravitational wave (GW) detectors are now operating around the world, including both laser interferometers [1, 2, 3, 4] and resonant mass detectors [5]. Combining the data from such a network of detectors can benefit both the detection of GW signals and estimation of signal parameters. Unlike real GW signals that would occur in coincidence across all detectors in a network, most background events due to instrumental and terrestrial disturbances are expected to be local to each detector and, therefore, can be rejected by analysing data from a network. Given a network with different orientations and locations of the detectors, GW sources can be localized on the sky and the waveforms of the two independent GW polarization components can be reconstructed.

Methods for the analysis of data from a network of GW detectors can be divided into two classes: *coincidence* and *coherent* methods. In coincidence methods, first, a search for GW signals is carried out for individual detectors and a list of candidate events is generated. Then a subset of events is selected by requiring temporal coincidence of events between the detectors. In coherent methods, one, first, combines the detector responses and then analyzes the combined data to generate a single list of events.

Networks of detectors are particularly important for searches of gravitational wave *burst* signals. These are defined to be broadband signals that may come either from unanticipated sources or from sources for which no reliable theoretical prediction exists for signal waveforms. Potential astrophysical sources of burst signals are stellar core collapse in Supernovae [6], mergers of binary neutron star or black hole systems [7] and Gamma Ray Burst progenitors [8].

The first coherent method for burst searches with a network of three misaligned detectors was proposed by Gürsel and Tinto [9]. In this method, the detector re-

sponses are combined into a functional, which attains its minimum at the correct direction to the source. The minimization of the functional allows one to reconstruct the source coordinates and two polarization waveforms of the burst signal.

Flanagan and Hughes [10] considered maximization of the *likelihood functional* [11, 12] as a means of reconstructing source direction and polarization waveforms. Anderson *et al* [13] extended this approach to derive a detection statistic called *excess power*. It is obtained by integrating the likelihood functional, weighted by a Bayesian prior probability density, over the space of all waveforms. In this paper, we refer to signal detection and reconstruction based on the global maximum of the unweighted likelihood functional as the *standard likelihood* method. Another coherent method, proposed by Sylvestre [14], starts with the *ad hoc* approach of forming a linear combination of data from a network of detectors. The combination coefficients are then adjusted to construct a quadratic detection algorithm that satisfies certain well defined criteria.

Arnaud *et al* [15] have numerically explored the issue of statistical performance of coherent and coincidence methods and find that the former are more efficient than the latter for burst signals. In the case of signals with known waveforms, Finn [16] has shown using simulations that a coherent method can also be robust when confronted with non-Gaussian noise.

Coherent methods can also be used for rejecting coincident background signals. Cadonati [17] has proposed a cross-correlation test, called *r-statistic*, for pairs of aligned detectors as a follow up consistency check on a coincidence analysis [18]. Rakhmanov and Klimenko [19] have proposed the *mixed correlations* method that extends the cross-correlation test to a network of three or more misaligned detectors. Wen and Schutz [20] have recently generalized the coherent approach of Gürsel and Tinto [9] to create a method for rejecting background coincident signals with a network of arbitrary detectors.

In this paper, we propose a method for the coherent de-

tection and reconstruction of burst signals that is based on the use of the likelihood ratio [11, 12]. Our analysis differs from [10, 13] in an important way. We identify and solve a problem with the standard likelihood analysis, first spotted in [21]. The problem, which we call the *two detector paradox*, is that the maximum likelihood ratio statistic for misaligned detectors does not reduce, contrary to physical intuition, to the statistic for co-aligned detectors in the limit of small misalignment angles. The latter statistic depends on the cross-correlation of detector outputs whereas the former does not. We show that the problem originates in the maximization of the likelihood ratio functional over all signal waveforms including those to which a detector network may not actually be sensitive. We propose a solution to this problem that is based on constraints imposed on the GW signal waveforms.

The constrained maximization of the likelihood functional yields new detection and reconstruction methods which we call the *constraint likelihood* methods. Unlike the Gürsel and Tinto method, the constraint likelihood methods can be used for arbitrary networks, including networks consisting of two detectors. The performance of these methods is studied in comparison with the standard likelihood method by using the numerical simulations. In the simulation we use networks of interferometric detectors consisting of LIGO 4 km detector in Hanford (H1), LIGO 4 km detector in Livingston (L1), GEO-600 detector (G1), TAMA detector (T1) and VIRGO detector (V1). We find that the constraints employed in this paper enhance the detection efficiency of the likelihood method. For detected sources, the constraints significantly improve accuracy of the source localization.

The rest of the paper is organized as follows. Section II lays out much of the basic notation and conventions used in the paper. In Section III, we provide an overview of the standard likelihood approach and its application to burst signals. Section IV describes the two detector paradox that appears in the standard likelihood approach. The origin of this problem is discussed in Section V. In Section VI we derive the constraint likelihood methods. The results from numerical studies of the performance of these methods are described in Section VII.

## II. DETECTOR RESPONSE TO GRAVITATIONAL WAVES

### A. Gravitational wave signal

Gravitational waves are described by a symmetric tensor of second rank  $h_{ij}(t)$ , which is usually defined in the transverse-traceless gauge [22]. It takes particularly simple form in the coordinate frame associated with the wave. In this coordinate frame (the wave frame), a gravitational wave propagates in the direction of  $z$  axis and it can be described with the waveforms  $h_+(t)$  and  $h_\times(t)$  representing two independent polarizations components

of the wave.

In addition to the waveforms  $h_+(t)$  and  $h_\times(t)$  we will use complex waveforms defined as

$$u(t) = h_+(t) + ih_\times(t), \quad (1)$$

$$\tilde{u}(t) = h_+(t) - ih_\times(t). \quad (2)$$

In what follows tilde will always denote complex conjugation. The GW waveforms  $u(t)$  and  $\tilde{u}(t)$  are eigenstates of the rotations around  $z$ -axis in the wave frame. We denote this particular rotation by  $R_z(\psi)$ , where  $\psi$  is the rotation angle. The rotation  $R_z(\psi)$  generates equivalent waveforms which are different representations of the same gravitational wave.

We define the sum-square energy [29] carried by the gravitational wave as

$$E = \int_{-\infty}^{\infty} (h_+^2(t) + h_\times^2(t)) dt = \int_{-\infty}^{\infty} u(t)\tilde{u}(t) dt. \quad (3)$$

Note that the sum-square energy is invariant under the rotation  $R_z$ .

### B. Detector response

The response of the interferometer to an arbitrary gravitational wave  $h_{ij}(t)$  is given by

$$\xi(t) = \frac{1}{2} T_{ij} h_{ij}(t), \quad (4)$$

where  $T_{ij}$  is the detector tensor [23]. In the wave frame the detector response is a linear superposition of two GW polarizations

$$\xi(t) = F_+ h_+(t) + F_\times h_\times(t). \quad (5)$$

where the coefficients  $F_+$  and  $F_\times$  are known as antenna patterns.

To calculate the antenna pattern we introduce the Earth-centered frame described in [24]. In this frame the detector location is defined by a radius-vector  $\mathbf{r}$  pointing to the detector and its orientation is described by two unit vectors  $\mathbf{a}$  and  $\mathbf{b}$  along the detector arms. The vectors  $\mathbf{a}$  and  $\mathbf{b}$  define the detector tensor

$$T'_{ij} = a_i a_j - b_i b_j, \quad i, j = 1, 2, 3, \quad (6)$$

where the indices correspond to spatial coordinates  $x$ ,  $y$  and  $z$  respectively. The direction to the GW source is defined in the Earth-centered frame by two spherical angles  $\phi$  (longitude) and  $\theta$  (latitude). The rotational transformation which connects the Earth-centered frame with the wave frame is given by

$$\mathbf{R}(\phi, \theta) = \mathbf{R}_y(\theta)\mathbf{R}_z(\phi). \quad (7)$$

It defines the detector tensor in the wave frame

$$\mathbf{T}(\phi, \theta) = \mathbf{R}(\phi, \theta) \mathbf{T}' \mathbf{R}(\phi, \theta)^T. \quad (8)$$

Omitting the explicit dependence on the angles, the antenna patterns corresponding to the  $h_+(t)$  and  $h_\times(t)$  polarizations are calculated as follows:

$$F_+ = \frac{1}{2}(T_{11} - T_{22}), \quad (9)$$

$$F_\times = \frac{1}{2}(T_{12} + T_{21}). \quad (10)$$

The detector response can be conveniently expressed in terms of the complex waveform  $u$ :

$$\xi = \tilde{A} u + A \tilde{u}, \quad (11)$$

where  $A$  and  $\tilde{A}$  are the complex antenna patterns:

$$A = \frac{1}{2}(F_+ + iF_\times), \quad (12)$$

$$\tilde{A} = \frac{1}{2}(F_+ - iF_\times). \quad (13)$$

A rotation  $R_z(\psi)$  in the wave frame induces the transformation of the detector antenna patterns and the GW waveforms

$$A' = e^{2i\psi} A, \quad (14)$$

$$u' = e^{2i\psi} u, \quad (15)$$

but the detector response is invariant under the rotation.

### III. LIKELIHOOD ANALYSIS OF GRAVITATIONAL WAVE DATA

In this section, we present a brief overview of the standard likelihood approach to the detection and reconstruction of gravitational wave burst signals using a network of detectors. Though the scientific content of this section is essentially the same as the results in [10, 13], our derivation and the notation we use are rather different. These will aid in a clearer exposition of our main results in subsequent sections. The reader is referred to [11] for a textbook level discussion of the statistical theory of signal detection used in this paper.

#### A. Overview

Consider an observable that is a finite data segment  $\mathbf{x} = \{x[1], x[2], \dots, x[N]\}$  from a noisy time series. The simplest detection problem is to define a *decision rule* for selecting one of two mutually exclusive hypotheses,  $H_0$  (*null hypothesis*) or  $H_1$  (*alternative hypothesis*), about the data  $\mathbf{x}$ . Under the  $H_0$  and  $H_1$ ,  $\mathbf{x}$  is a realization of a stochastic process described by the joint probability density  $p(\mathbf{x}|H_0)$  and  $p(\mathbf{x}|H_1)$  respectively.

Any decision rule will incur two types of errors: *false alarm* -  $H_1$  is selected when  $H_0$  is true, and *false dismissal* -  $H_0$  is selected when  $H_1$  is true. Each error will have a probability associated with it, namely, the false alarm

and the false dismissal probabilities  $Q_0$  and  $Q_1$  respectively. In order to select the best decision rule, several criteria have been proposed out of which the Neyman-Pearson criterion is the most suitable for detection of gravitational waves. According to this criterion, the optimal decision rule has the least  $Q_1$  for fixed  $Q_0$ . The rule accepts  $H_1$  ( $H_0$ ) when the *likelihood ratio*,  $\Lambda(\mathbf{x})$ , defined as

$$\Lambda(\mathbf{x}) = \frac{p(\mathbf{x}|H_1)}{p(\mathbf{x}|H_0)}, \quad (16)$$

is greater (less) than a threshold value that is fixed by the specified  $Q_0$ .

In the case of the GW data analysis,  $H_0$  is the hypothesis “a GW signal is absent” and  $H_1$  is “the GW signal  $\xi$  is present”. For a stationary, Gaussian white noise with zero mean the corresponding joint probability densities are

$$p(\mathbf{x}|H_0) = \prod_{i=1}^N \frac{1}{\sqrt{2\pi}\sigma} \exp\left(-\frac{x^2[i]}{2\sigma^2}\right), \quad (17)$$

$$p(\mathbf{x}|H_1) = \prod_{i=1}^N \frac{1}{\sqrt{2\pi}\sigma} \exp\left(-\frac{(x[i] - \xi[i])^2}{2\sigma^2}\right), \quad (18)$$

where  $\sigma$  is the standard deviation of the noise. The logarithm of the likelihood ratio can be expressed as

$$\mathcal{L} = \ln(\Lambda(\mathbf{x})) = \sum_{i=1}^N \frac{1}{\sigma^2} \left( x[i]\xi[i] - \frac{1}{2}\xi^2[i] \right). \quad (19)$$

In the rest of the paper, we will be concerned only with  $\mathcal{L}$  which will be referred to as simply the *likelihood*.

The situation with two mutually exclusive hypotheses, outlined above, is the simplest one. In general, as in the case of GW analysis, the observed data  $\mathbf{x}$  can be a realization of one among several joint probability densities  $p(\mathbf{x}|H_i)$ ,  $i = 0, 1, 2, \dots$ , where, as usual,  $H_0$  is the null hypotheses and  $H_i$  are the alternative hypotheses. Correspondingly, the probabilities for false alarm and false dismissal can be assigned but now the false dismissal probabilities  $Q_i$  are hypothesis specific.

One possible generalization of the Neyman-Pearson criterion could be to select that decision rule which minimizes all probabilities  $Q_i$  for a fixed false alarm probability  $Q_0$ . It turns out that, in general, no such rule is possible [11]. Another approach is to generalize the likelihood ratio test itself by constructing a functional

$$\Lambda_m(\mathbf{x}) = \max_i \left[ \frac{p(\mathbf{x}|H_i)}{p(\mathbf{x}|H_0)} \right], \quad (20)$$

and comparing it with a threshold. This test, called the maximum likelihood ratio (MLR) test, tends to outperform any other *ad hoc* test. However, it is important to note that the MLR test itself does not have a formal proof of optimality. Therefore, it is possible that modifications

of the MLR test, as presented in this paper, can lead to better performance.

One of the applications of the MLR test is the detection of gravitational waves from the inspiral of compact binaries [16, 25]. In principle, the waveforms of the GW signals can be calculated to arbitrary precision given the parameters of the binary system. The set of alternative hypotheses now becomes a continuum that is identified with the space of binary parameters. The likelihood ratio  $\Lambda(\mathbf{x}|H_i)$  can, therefore, be expressed as a function over the binary parameters. The MLR statistic is obtained by maximizing the likelihood ratio over these parameters and reaches its maximum for the best match of the corresponding waveform to the data.

In contrast to binary inspiral signals, where the number of parameters is small, the parameters characterizing burst signals are essentially the signal amplitudes themselves at each instant of time. Thus, for burst signals, the number of parameters can be very large. Formally, however, the concept of the likelihood ratio can still be used for burst signals. In this case, the likelihood ratio is  $\Lambda(\mathbf{x}|\xi)$ , where  $\xi$  is the detector response to the burst signal. The application of the MLR test to burst signals involves maximization over each sample  $\xi[i]$  independently [26].

## B. Network likelihood

So far, we have considered a time series  $\mathbf{x}$  at the output of a single GW detector. The entire formalism outlined above can be extended to a network of detectors. Let the data from the  $k^{\text{th}}$  detector be  $\mathbf{x}_k = \{x_k[1], x_k[2], \dots\}$  and the detector response to the gravitational wave be

$$\xi_k[i] = u[i]\tilde{A}_k + \tilde{u}[i]A_k. \quad (21)$$

We will assume that the noise in different detectors is independent. Then the likelihood ratio becomes,

$$\mathcal{L} = \sum_{k=1}^K \sum_{i=1}^N \frac{1}{\sigma_k^2} \left( x_k[i]\xi_k[i] - \frac{1}{2}\xi_k^2[i] \right). \quad (22)$$

where  $K$  is the number of detectors in the network. For detectors illuminated by the same GW source, the detector responses are not independent. Therefore, the variation of the likelihood functional is performed over the sampled amplitudes  $u[i]$  and  $\tilde{u}[i]$ .

To characterize the angular and strain sensitivity of the network, we introduce the *network antenna patterns*

$$g_r = \sum_{k=1}^K \frac{A_k \tilde{A}_k}{\sigma_k^2}, \quad g_c = \sum_{k=1}^K \frac{A_k^2}{\sigma_k^2}, \quad (23)$$

where  $g_r$  is real and  $g_c$  is complex. Similarly to the antenna patterns  $A_k$  for a single detector, they describe the *network response* to the gravitational wave:

$$R(u) = g_r u + g_c \tilde{u}. \quad (24)$$

We also define the network output time series  $X$  which combines the output time series  $\mathbf{x}_k$  from individual detectors

$$X = \sum_{k=1}^K \frac{\mathbf{x}_k A_k}{\sigma_k^2}. \quad (25)$$

To simplify equations, we will replace summation over any sampled time series  $s[i]$  with  $\langle s \rangle$ . With these new notations the likelihood functional can be written as

$$\mathcal{L} = \left\langle u\tilde{X} + \tilde{u}X - g_r u\tilde{u} - \frac{\tilde{g}_c u^2 + g_c \tilde{u}^2}{2} \right\rangle, \quad (26)$$

where the  $\tilde{X}$  and  $\tilde{g}_c$  are complex conjugates of  $X$  and  $g_c$  respectively.

## C. Solution for GW waveforms

The equations for the GW waveforms are obtained by variation of the likelihood functional:

$$\frac{\delta \mathcal{L}}{\delta u} = 0, \quad \frac{\delta \mathcal{L}}{\delta \tilde{u}} = 0, \quad (27)$$

which results in two linear equations for  $u$  and  $\tilde{u}$

$$X = g_r u + g_c \tilde{u}, \quad (28)$$

$$\tilde{X} = g_r \tilde{u} + \tilde{g}_c u. \quad (29)$$

The solution is

$$u_s = \frac{g_r X - g_c \tilde{X}}{g_r^2 - |g_c|^2}. \quad (30)$$

Note, the solution  $u_s$  satisfies the condition  $X = R(u_s)$ , where  $R(u_s)$  is the network response to the gravitational wave (see Eq.(24)). Equations 28 and 29 can also be written in the matrix form

$$\begin{bmatrix} \text{Re}(X) \\ \text{Im}(X) \end{bmatrix} = M_R \begin{bmatrix} h_+ \\ h_\times \end{bmatrix}, \quad (31)$$

where the matrix  $M_R$  is given by

$$M_R = \begin{bmatrix} g_r + \text{Re}(g_c) & \text{Im}(g_c) \\ \text{Im}(g_c) & g_r - \text{Re}(g_c) \end{bmatrix}. \quad (32)$$

## D. Maximum likelihood ratio statistic

The maximum likelihood ratio statistic is obtained by substitution of the solution  $u_s$  in Eq.(26)

$$L_{\text{max}} = \frac{2g_r X_r - \tilde{g}_c X_c - g_c \tilde{X}_c}{2(g_r^2 - |g_c|^2)}, \quad (33)$$

where the quantities  $X_c$  and  $X_r$  are defined by

$$X_c = \sum_{i=1}^K \sum_{j=1}^K A_i A_j D_{ij}, \quad (34)$$

$$X_r = \sum_{i=1}^K \sum_{j=1}^K A_i \tilde{A}_j D_{ij}, \quad (35)$$

and  $\tilde{X}_c$  is complex conjugate of  $X_c$ . The data matrix  $D_{ij}$  is calculated for the detector output  $x_i$  and  $x_j$  scaled by the variances of the detector noise

$$D_{ij} = \frac{\langle x_i(t)x_j(t + \tau_{ij}) \rangle}{\sigma_i^2 \sigma_j^2}. \quad (36)$$

The data matrix depends on the gravitational wave time delays  $\tau_{ij}$  between the detectors. The time delays, in turn, depend on the coordinates of the source on the sky  $\theta$  and  $\phi$ . The diagonal elements of the data matrix represent the power terms and the non-diagonal elements represent the cross-correlation terms.

There is a simple geometrical interpretation of the MLR statistics. At any instance of time, the GW waveform  $u$  and the network output  $X$  can be viewed as vectors  $\mathbf{u}$  and  $\mathbf{X}$  in the complex plane. Then the MLR statistics, given by Eq.(33), is the inner product

$$L_{\max} = \frac{1}{2} \langle u_s \tilde{X} + \tilde{u}_s X \rangle = \langle \mathbf{u}_s \cdot \mathbf{X} \rangle, \quad (37)$$

which is a projection of the solution  $u_s$  onto the data  $X$ . Note, that the projection is the estimator of the total signal-to-noise ratio of the GW signal detected in the network

$$\text{SNR}_{\text{tot}} = \sum_{k=1}^K \frac{\langle \xi_k^2 \rangle}{\sigma_k^2} \approx 2 \langle \mathbf{u}_s \cdot \mathbf{X} \rangle. \quad (38)$$

#### IV. TWO DETECTOR PARADOX

So far we have described the standard likelihood approach for the detection and reconstruction of burst GW signals wherein the likelihood ratio is maximized independently over each signal sample. Though attractive because both a detection and estimation method are obtained simultaneously, there is a problem with this approach when applied to a network of two detectors. The problem, which we call the *two-detector paradox*, is described in this section.

Let us consider a network of two detectors in two configurations: (A) aligned detectors and (M) misaligned detectors. The detectors in the configuration A have the same antenna patterns. In this case the detector responses are the same in both detectors and we consider the GW signal as the scalar wave  $\xi$ . The likelihood functional is then

$$\mathcal{L}_A = \frac{\langle x_1 \xi \rangle}{\sigma_1^2} + \frac{\langle x_2 \xi \rangle}{\sigma_2^2} - \frac{\langle \xi^2 \rangle}{2} \left( \frac{1}{\sigma_1^2} + \frac{1}{\sigma_2^2} \right), \quad (39)$$

where  $x_1, x_2$  are the detector outputs and  $\sigma_1, \sigma_2$  are the standard deviations of the detector noise. The solution of the likelihood variation problem is

$$\xi = \left( \frac{x_1}{\sigma_1^2} + \frac{x_2}{\sigma_2^2} \right) \left( \frac{1}{\sigma_1^2} + \frac{1}{\sigma_2^2} \right)^{-1}. \quad (40)$$

The MLR statistics for two aligned detectors is obtained from Eq.(39) by substituting  $\xi$  with the solution

$$L_A = \frac{1}{2} \left( \frac{\langle x_1^2 \rangle}{\sigma_1^4} + \frac{\langle x_2^2 \rangle}{\sigma_2^4} + 2 \frac{\langle x_1 x_2 \rangle}{\sigma_1^2 \sigma_2^2} \right) \left( \frac{1}{\sigma_1^2} + \frac{1}{\sigma_2^2} \right)^{-1}. \quad (41)$$

As expected, the MLR statistic for two aligned detectors includes both the power and the cross-correlation terms. For two arbitrary misaligned detectors the MLR statistic, given by Eq.(33), reduces to

$$L_M = \frac{1}{2} \left( \frac{\langle x_1^2 \rangle}{\sigma_1^2} + \frac{\langle x_2^2 \rangle}{\sigma_2^2} \right). \quad (42)$$

which includes the power terms only.

The two detector paradox is that the statistic  $L_M$  does not include cross-correlation between the detectors even for a small misalignment. This is highly counterintuitive since one expects that the response of detectors to the same GW source will differ only infinitesimally when the detectors are infinitesimally misaligned. Hence, as in the case of  $L_A$ , one would expect that the cross-correlation term will benefit detection and that its importance will decline only gradually as the detectors are misaligned. In other words, the functional  $L_M$  is expected to approach  $L_A$  in the limit of perfect alignment.

The origin of the two detector paradox is easily seen. For the aligned case, the standard likelihood ratio approach has the prior information that both detector responses are identical. Hence, the cross-correlation term is guaranteed to have positive mean and, thus, should improve the detectability of GW signals. While, for the misaligned case, it is always possible to specify two arbitrary responses and invert them to obtain some  $h_+(t)$  and  $h_\times(t)$  components of the GW signal. The standard MLR statistic, therefore, does not benefit from having the cross-correlation term since now it can contribute pure noise to the statistic. Hence, this term disappears from the MLR statistic. The fact that the standard likelihood approach does not exhibit the expected continuity for the case of two detectors indicates that this approach may not be the best one for a general network of GW detectors also.

#### V. NETWORK RESPONSE

To resolve the two detector paradox we take a closer look at how the GW signal and the detector noise contribute to the MLR statistic. In this section we show

that the detection of two GW components can be considered as two independent measurements equally affected by the detector noise but conducted with different angular and strain sensitivities of the detectors. Being an *ad hoc* method, the maximum likelihood may not be an optimal approach in this situation. For example, if the network is sensitive only to one signal component (as in the case of co-aligned detectors) the measurement of the second component does not benefit the GW detection, but rather adds noise to the measurement. In the next section we propose a solution to the problem and derive the detection statistics, which continuously bridge the cases of aligned and misaligned detectors.

### A. Network response to gravitational waves

As we mentioned in Section II B, the detector response is invariant under rotations  $R_z$  in the wave frame. Consequently, all measurable quantities, including the likelihood functional, are invariant as well. We have a freedom to select an arbitrary wave frame by applying the rotation  $R_z(\psi)$ , where  $\psi$  is the rotation angle. The rotation induces the transformation of the GW waveforms and the detector antenna patterns (see Eq.(14)), as well as the transformation of the network parameters:  $X \rightarrow X e^{i2\psi}$  and  $g_c \rightarrow g_c e^{i4\psi}$ . In general, the rotation angle  $\psi$  can be selected individually for each instance of time and for each point in the sky. By applying the rotation  $R_z(-\gamma/4)$ , where  $\gamma$  is the phase of  $g_c$ , we selected a wave frame in which both network antenna patterns are real and positively defined. We call this particular coordinate frame the dominant polarization frame .

As follows from Eq.(24), for a GW signal  $u$  defined in the dominant polarization frame, the network response is

$$R = (g_r + |g_c|) h_1 + i(g_r - |g_c|) h_2 , \quad (43)$$

where  $h_1$  and  $h_2$  are the real and imaginary components of the signal. We will distinguish them from the GW polarizations  $h_+$  and  $h_\times$  defined for an arbitrary wave frame. Note, the coefficients in front of  $h_1$  and  $h_2$  are the eigenvalues of the network response matrix  $M_R$  (Eq.(32)), which takes a diagonal form in the dominant polarization frame

$$M_R = g \begin{pmatrix} 1 & 0 \\ 0 & \epsilon \end{pmatrix} . \quad (44)$$

The coefficient

$$g = g_r + |g_c| \quad (45)$$

characterizes the network sensitivity to the  $h_1$  wave. The sensitivity to the second component  $h_2$  is  $\epsilon g$ , where  $\epsilon$  is the network alignment factor:

$$\epsilon = \frac{g_r - |g_c|}{g_r + |g_c|} . \quad (46)$$

The alignment factor  $\epsilon$  shows the relative sensitivity of the network to the GW components  $h_1$  and  $h_2$ . Note that  $0 \leq \epsilon \leq 1$ . The total signal-to-noise ratio of the GW signal detected in the network is

$$\text{SNR}_{\text{tot}} = 2g (\langle h_1^2 \rangle + \epsilon \langle h_2^2 \rangle) , \quad (47)$$

where  $\langle h_1^2 \rangle$  and  $\langle h_2^2 \rangle$  are the sum-square energies carried by each component (see Eq.(3)). Therefore, to be detected with the same signal-to-noise ratio, the  $h_2$  wave should carry  $1/\epsilon$  times more energy than the  $h_1$  wave.

Both the network sensitivity and the alignment factor depend on the angular and the strain sensitivities of the detectors. The alignment factor reflects also the angular alignment of the detectors. For co-aligned detectors  $\epsilon = 0$  and the  $h_2$  component of the GW signal can not be detected. Even for detectors with large angular misalignment, depending on the sky coordinates  $\theta$  and  $\phi$ , the alignment factor may take small values indicating that the detectors are effectively aligned. For example, Figure 1 shows the alignment factors as a function of the sky coordinates calculated for several network configurations consisting of the H1, L1, G1, V1 and T1 detectors. For simplicity, we assume that the detectors have the same strain sensitivity. The example shows, that for the closely aligned H1-L1 detectors, the alignment factor is close to zero everywhere, except for a few small patches on the sky. The more detectors are added to the network, the larger is the area on the sky with large values of  $\epsilon$ . But even for the network of five detectors (H1-L1-G1-V1-T1), the factor  $\epsilon$  remains small for a considerable fraction of the sky area, where the network is much less sensitive to the  $h_2$  wave, than to the  $h_1$  wave. Assuming that both components carry on average the same energy, the  $h_2$  wave is suppressed by the factor of  $\epsilon$ . Therefore, the  $h_2$  component adds little to the total signal-to-noise ratio  $\text{SNR}_{\text{tot}}$  for GW signals originating from areas on the sky with small values of  $\epsilon$ .

The coefficient  $g$  defines the overall sensitivity of the network to the gravitational waves. Figure 2 shows the network sensitivity calculated as a function of the sky coordinates for several network configurations. As we expect, adding more detectors reduces the sky area where the network is blind to gravitational waves.

### B. Two components of the likelihood functional

In the dominant polarization frame the likelihood functional can be written as

$$\mathcal{L}(u) = \left\langle u \tilde{X}_\gamma + \tilde{u} X_\gamma - g_r u \tilde{u} - \frac{|g_c|}{2} (u^2 + \tilde{u}^2) \right\rangle . \quad (48)$$

where  $X_\gamma = X e^{-i\gamma/2}$ . Expressed in terms of  $h_1$  and  $h_2$ , it can be written as  $\mathcal{L}(h_1, h_2) = \mathcal{L}_1(h_1) + \mathcal{L}_2(h_2)$ :

$$\mathcal{L}_1 = 2 \left\langle |X| \cos(\beta) h_1 - \frac{g}{2} h_1^2 \right\rangle , \quad (49)$$

$$\mathcal{L}_2 = 2 \left\langle |X| \sin(\beta) h_2 - \frac{\epsilon g}{2} h_2^2 \right\rangle , \quad (50)$$

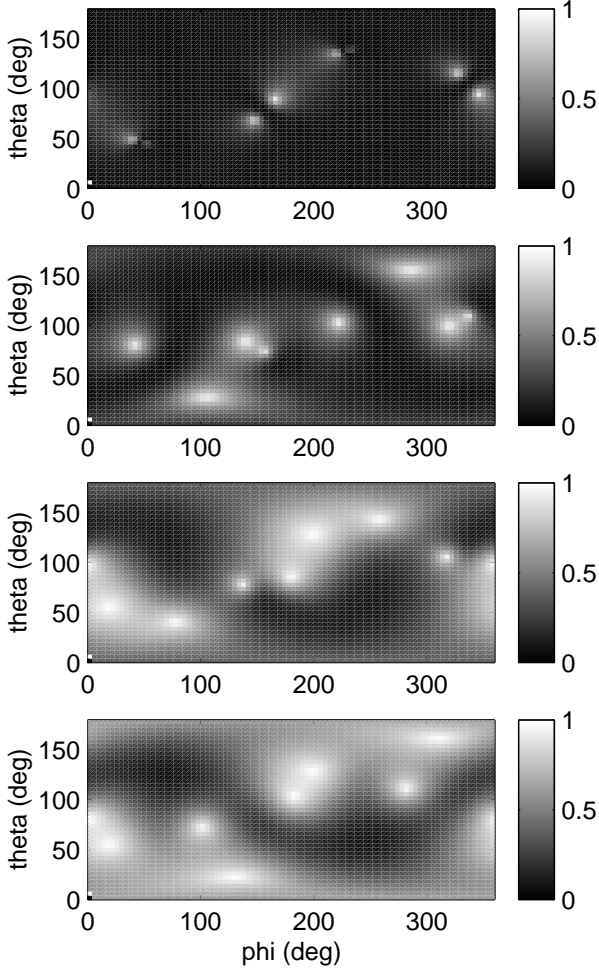


FIG. 1: Alignment factors for the detector networks listed in the order from top to bottom: H1-L1 (upper plot), H1-L1-G1, H1-L1-G1-V1, H1-L1-G1-V1-T1 (bottom plot).

where  $|X|$  is the amplitude and  $\beta$  is the phase of the data vector  $X_\gamma$ . The solutions for the  $h_1$  and  $h_2$  are obtained by the variation of the  $\mathcal{L}_1$  and  $\mathcal{L}_2$  functionals:

$$h_1 = \frac{1}{g}|X| \cos(\beta), \quad h_2 = \frac{1}{\epsilon g}|X| \sin(\beta), \quad (51)$$

The MLR statistic can be calculated separately for each component

$$L_1 = \frac{1}{g} \langle |X|^2 \cos^2(\beta) \rangle = \frac{2X_r + e^{-i\gamma}X_c + e^{+i\gamma}\tilde{X}_c}{4g}, \quad (52)$$

$$L_2 = \frac{1}{\epsilon g} \langle |X|^2 \sin^2(\beta) \rangle = \frac{2X_r - e^{-i\gamma}X_c - e^{+i\gamma}\tilde{X}_c}{4\epsilon g}. \quad (53)$$

The statistics  $L_1$  and  $L_2$  are the estimators of the signal-to-noise ratio of two GW components detected in the network.

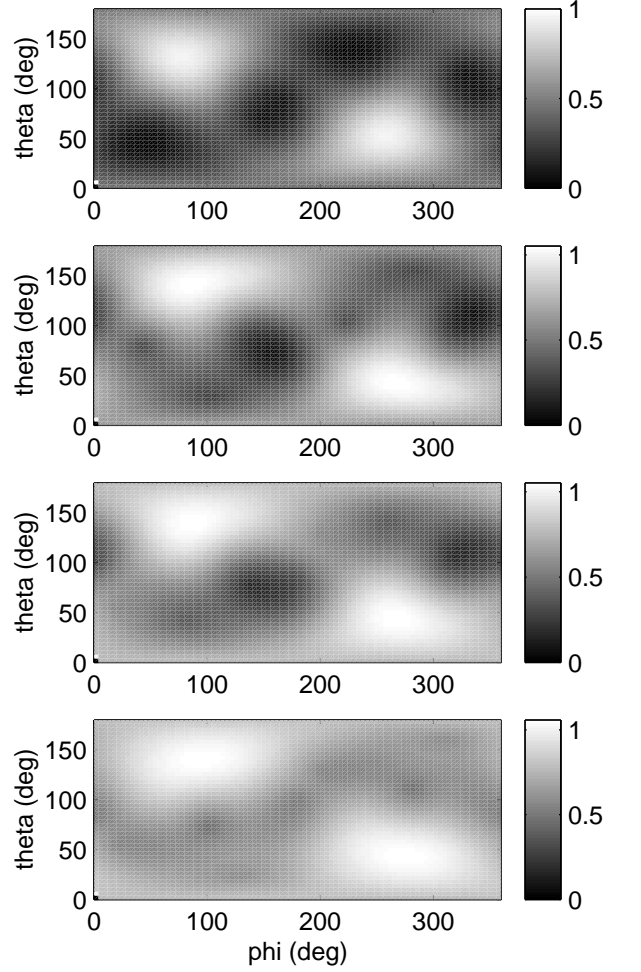


FIG. 2: Sensitivity of the detector networks listed in the order from top to bottom: H1-L1 (upper plot), H1-L1-G1, H1-L1-G1-V1, H1-L1-G1-V1-T1 (bottom plot).

### C. Detector noise

The detector output  $x_k$  is a sum of the detector noise  $n_k$  and the detector response  $\xi_k$ . If no GW signal is present than the network output is

$$X_n = \sum_{k=1}^K \frac{n_k A_k}{\sigma_k^2}, \quad (54)$$

which follows from the definition of the data vector  $X$  (see Eq.(25)). In this case, as follows from Eq.(30), the likelihood variation procedure produces the non-zero solutions  $u_s$  for the GW waveforms and the MLR statistic is the biased estimator of  $\text{SNR}_{\text{tot}}$ . The reconstructed sum-square energy

$$E_n = \langle h_{1n}^2 \rangle + \langle h_{2n}^2 \rangle = \frac{1}{g} \left( L_{1n} + \frac{L_{2n}}{\epsilon} \right), \quad (55)$$

is biased as well, where  $L_{1n}$  and  $L_{2n}$  are the MLR statistics due to the detector noise. The ensemble average  $\overline{E_n}$  can be easily calculated when the detector noise is white and Gaussian. Indeed, in this case the mean of the data matrix is

$$\overline{D_{ij}} \propto \frac{\delta_{ij}}{\sigma_i \sigma_j}, \quad (56)$$

where  $\delta_{ij}$  is the Kronecker delta. The average MLR statistics due to the detector noise is than

$$\overline{L_{1n}} = \overline{L_{2n}} \propto 1/2. \quad (57)$$

As one can see, in average the detector noise introduces the same bias for each signal component. From Eq.(55) it follows that the reconstructed energy in the second component is proportional to  $1/\epsilon$  and it diverges when  $\epsilon \rightarrow 0$ . Therefore, for small values of  $\epsilon$ , the likelihood variation procedure may result in the un-physical solutions for the signal component  $h_2$ . This is the root of the two detector paradox described in Section IV.

The statistics  $L_1$  and  $L_2$  can be considered as two independent measurements of the GW components  $h_1$  and  $h_2$ . Indeed, the measurements are uncorrelated, and their fluctuations are characterized by the same variances of the noise, which follows from the equations

$$\overline{(L_{1n} - \overline{L_{1n}})(L_{2n} - \overline{L_{2n}})} = 0, \quad \overline{L_{1n}^2} = \overline{L_{2n}^2}. \quad (58)$$

When the value of the alignment factor is small, the standard MLR statistic  $L_{\max}$  is not the optimal estimator of  $\text{SNR}_{\text{tot}}$ , because the second component adds pure noise into the measurement.

## VI. CONSTRAINT LIKELIHOOD

We have seen that for the standard likelihood approach the problem arises when there is a large asymmetry ( $\epsilon \ll 1$ ) in the detection of two GW components. In this case we could find better estimators for the GW waveforms and for the total signal-to-noise ratio of the GW signal detected in the network. The construction of such estimators depend on our assumptions about the GW signals. Mathematically these assumptions can be implemented as constraints applied to the likelihood functional. The purpose of the constraints is to exclude the un-physical solutions arising from the variation of the likelihood functional. By removing such solutions from the waveform parameter space we expect to sacrifice a small fraction of the real GW signals, while considerably improve the detection for the rest of the sources. Below we consider examples of the likelihood constraints that can be used in the analysis.

### A. Hard constraint

Given a source population, we could expect that in average both signal components  $h_1$  and  $h_2$  carry about the

same energy. For example, for binary sources, the gravitational waves are emitted with the random inclination angles. For waves in the dominant polarization frame, which is oriented randomly with respect to the source frame, the ensemble mean of the sum-square energies of two components satisfies

$$\overline{\langle h_1^2 \rangle} = \overline{\langle h_2^2 \rangle}. \quad (59)$$

For areas in the sky where the network alignment factor is small, for most of the sources the detected energy will be dominated by the first component (see Eq.(47)). For example, for a network consisting of three interferometric detectors H1, L1 and G1 the alignment factor is less than 0.1 for approximately 50% of the sky area. Therefore, the noisy component  $h_2$  can be entirely ignored for those sky locations where  $\epsilon$  is less than some threshold  $\epsilon_0$ . This requirement impose a constraint on the reconstructed GW waveforms and, therefore, on the MLR statistic. For a given sky location we define the *hard* MLR statistic as

$$L_{\text{hard}} = \begin{cases} L_1 & \epsilon < \epsilon_0, \\ L_{\max} & \epsilon \geq \epsilon_0. \end{cases} \quad (60)$$

When the threshold  $\epsilon_0 = 1$ , the MLR statistics is defined by the first signal component only. In the limit of a small alignment angle between the detectors ( $\epsilon \rightarrow 0$ ), the hard constraint statistics converges to the statistics for co-aligned detectors thus resolving the two detector paradox.

The hard constraint is a good approximation in the case of closely aligned detectors, such as the network of the H1-L1 detectors. The simulation results (see Section VII) show, that the  $L_1$  is a reasonably good statistic even for a network of the H1-L1-G1 detectors with large angular misalignment between the LIGO and GEO detectors. However, if the detection statistic  $L_1$  is used, the search algorithm is entirely inefficient to a GW signal when  $h_1 = 0$ . Although, such GW signals are quite unlikely (due to random relative orientations of the source and the dominant polarization frames), and for small values of  $\epsilon$  they may not be detected anyway (unless the  $h_2$  component is very strong), in the next section we introduce a different constraint, which is free from this problem.

### B. Soft constraint

As we mentioned in Section VB, the unconstrained MLR statistic  $L_{\max}$  is a sum of the statistics  $L_1$  and  $L_2$ , which can be written as

$$L_{\max} = \frac{1}{g} \langle |X|^2 (1 + \delta) \rangle, \quad \delta = \frac{1 - \epsilon}{\epsilon} \sin^2(\beta). \quad (61)$$

If the detector output is dominated by the GW signal, and assuming that both GW components carry about the



same energy, the ensemble average for  $\sin^2(\beta)$  is

$$\overline{\sin^2(\beta)} \approx \epsilon^2 / (1 + \epsilon^2), \quad (62)$$

which follows from the expression for the network response (see Eq.(43)). It means that in average

$$\bar{\delta} \approx \epsilon \frac{1 - \epsilon}{1 + \epsilon^2} \quad (63)$$

and the second term in Eq.(61) is much less than 1. On contrary, for the detector noise

$$\overline{\sin^2(\beta)} \approx \epsilon \quad (64)$$

and respectively

$$\bar{\delta} \approx 1 - \epsilon. \quad (65)$$

Therefore, the noisy second term in Eq.(61) can be omitted, resulting in the statistic, which we call the *soft* MLR statistic

$$L_{\text{soft}} = \frac{1}{g} \langle |X|^2 \rangle = L_1 + \epsilon L_2. \quad (66)$$

There is a simple statistical justification of this result. Since the statistics  $L_1$  and  $L_2$  are two uncorrelated Gaussian random variables with the mean  $\mu_1$  and  $\mu_2$ , and the variance  $\nu$ , the joint probability  $P(L_1, L_2, \mu_1, \mu_2, \nu)$  belongs to the Rayleigh distribution. For the assumption above (see Eq.(59)), we expect that  $\mu_1 = gE$  and  $\mu_2 = \epsilon gE$ , where  $E$  is the GW sum-square energy. Then the best estimator for  $\text{SNR}_{\text{tot}}$  is obtained by maximizing  $P$  over  $E$ , which gives the statistic  $L_{\text{soft}}$ .

To obtain the solution for the GW waveforms, one should impose a constraint on the likelihood functional itself. The constraint can be integrated into the variation procedure by the method of the Lagrange multiplier [27]. In this method, first, we have to obtain the constraint equation. The soft constraint can be constructed by requiring that

$$g \langle h_1^2 \rangle + \epsilon g \langle h_2^2 \rangle = 0, -\frac{1}{g} \langle |X|^2 \rangle. \quad (67)$$

which limits the sum-square energies  $\langle h_1^2 \rangle$  and  $\langle h_2^2 \rangle$ . Since, the constraint is applied to the  $h_2$  component only, we can replace the  $h_1$  with the solution for the first component and re-write the constraint as

$$\epsilon g \langle h_2^2 \rangle - \frac{1}{g} \langle |X|^2 \sin^2(\beta) \rangle = 0. \quad (68)$$

The solution for the second GW component  $h_2$  is trivially obtained by the constraint variation of the likelihood functional  $\mathcal{L}_2$

$$h_{2\text{soft}} = \frac{1}{\sqrt{\epsilon g}} |X| \sin(\beta). \quad (69)$$

As one can see, the constrained solution is the standard solution  $h_2$ , multiplied by a penalty factor of  $\sqrt{\epsilon}$ , which

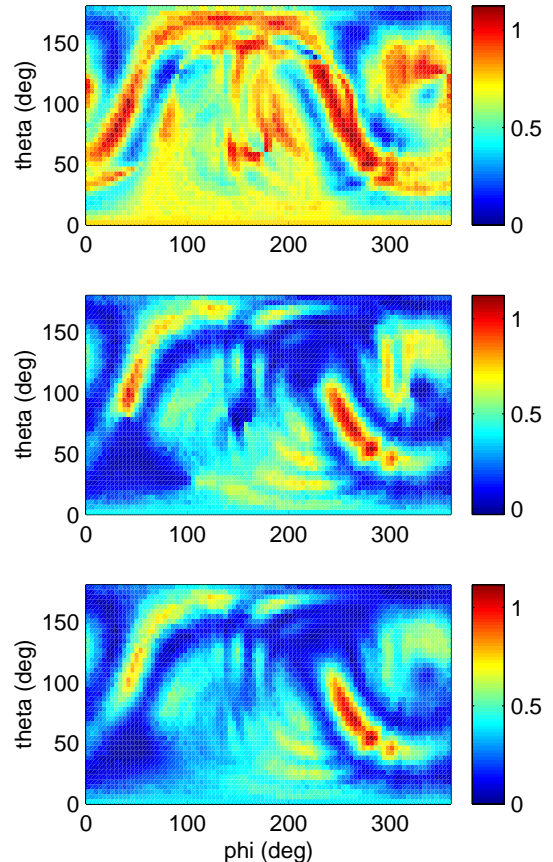


FIG. 3: Sky maps of the likelihood statistics  $L_{\text{max}}$  (top),  $L_{\text{hard}}$  (middle) and  $L_{\text{soft}}$  (bottom) for the detector network H1-L1-G1. The injected signal SNR is 17 (H1), 20 (L1) and 9 (G1). The source is located at  $\theta = 50^\circ$  and  $\phi = 280^\circ$ .

reduces both the noise and the signal contribution from the second component to the MLR statistic at small values of  $\epsilon$ . Obviously, it reduces the sensitivity of the  $L_{\text{soft}}$  statistic to a particular class of GW signals with  $h_1 = 0$ , described in Section VIA. For these signals, to be detected with the same false alarm rate, the  $L_{\text{soft}}$  statistic requires  $(1 + \epsilon^2)/2\epsilon$  times more powerful GW signal, than the standard  $L_{\text{max}}$  statistic. For example, for  $\epsilon = 0.1$  the degradation of the strain sensitivity is by a factor of 2. But it happens only for a small fraction of the GW sources. Compare to the standard likelihood method, for most of the sources we expect to improve the detection sensitivity if the  $L_{\text{soft}}$  statistic is used.

### C. Network sky maps

In un-triggered burst searches the coordinates of the source,  $\theta$  and  $\phi$  are free parameters. In this case, the detector responses, the likelihood statistics and the reconstructed waveforms become functions of  $\theta$  and  $\phi$  or

skymaps. For example, the skymaps corresponding to different statistics are shown in Figure 3. (For details see Section VII).

For a given location in the sky, the value of the likelihood statistic indicates how consistent the data is with the hypothesis that a GW signal originates from that location. The coordinates  $\theta$  and  $\phi$  which yield maximum for the likelihood statistic correspond to the most probable location of the source. The maximum value of the statistic is then used for detection. By setting a threshold on the maximum likelihood value one can decide on the presence or absence of a gravitational wave signal in the data as described in Section III. Given the most probable source coordinates the waveforms  $h_+(t)$  and  $h_\times(t)$  are reconstructed as described in Section VI.

## VII. NUMERICAL SIMULATION

We have outlined a general method for using the MLR statistic in conjunction with constraints limiting the space of the GW waveforms. The method is intended for application to burst searches with networks of gravitational wave detectors. The performance of the method and the effect of the constraints can be analyzed using numerical simulations with modeled waveforms. The present simulation is similar to the one previously used for estimating the performance of the mixed correlation method [19].

### A. Simulation procedure

The two-polarization waveforms which represent burst gravitational waves used in the simulation are taken from the numerical models of the merger phase of coalescing binary black holes (BH) [28]. These waveforms form a one-parameter family BH- $M$ , where  $M$  is the total mass of the binary system in units of solar mass. The results below correspond to  $M = 100$ . In the simulations we generate the detector noise which is Gaussian and white. The variance of the noise is selected to be the same for all detectors.

A typical simulated data segment has the duration of 1 second and consists of  $N = 4096$  data samples. For calculation of the data matrix (see Eq.(36)) we set the integration window of 85 ms, which is substantially greater than the duration of the signal. The magnitude of the simulated signals is controlled by the overall gain  $G$ , which is varied from 0 to 10, whereas the magnitude of the noise is kept fixed.

Due to different orientation of the detectors with respect to the incoming gravitational wave, the detectors responses are different (see Eq.(11)). To characterize the magnitude of the signal in any given detector we define

the signal-to-noise ratio:

$$\text{SNR} = \int_{-\infty}^{\infty} \frac{|\xi(f)|^2}{S(f)} df \rightarrow \frac{1}{\sigma^2} \sum_{i=0}^{N-1} \xi^2(t_i), \quad (70)$$

where  $S(f)$  is the power spectral density of the noise. For white Gaussian noise  $S(f) = \sigma^2/f_s$ , where  $f_s$  is the sampling rate.

For any given detector in the network, the magnitude of the signal varies significantly depending on the source location in the sky. We therefore choose the location of the simulated sources at random, with a uniform distribution over the sky. We also choose the polarization angle  $\psi$  at random from the interval  $[0^\circ, 360^\circ]$ . With these choices the simulation gives us an estimate of the performance of the detection algorithms without the bias which can be introduced by the particular choice for the source location or its polarization angle.

The simulation consists of series of tests corresponding to different values of SNR (controlled by  $G$ ). For each value of  $G$  a total number of 10,000 injections were made. To characterize the strength of the signal in each detector for the entire test we introduce the sky-average SNR, denoted by  $\overline{\text{SNR}}$ . The sky-average SNR is proportional to  $G$  and it is the same for each detector in the network ( $\overline{\text{SNR}} \approx 2.3G$ ).

### B. Simulation results

In the simulation we tested the following detection methods: the standard likelihood method ( $L_{\text{max}}$ ), the hard constraint method ( $L_{\text{hard}}$ ), and the soft constraint method ( $L_{\text{soft}}$ ). The detection performance of the methods is compared by using the receiver operating characteristic (ROC), which shows the detection probability as a function of the false alarm probability. Examples of the ROC curves, corresponding to  $G = 3$  and  $G = 4$ , are shown in Figure 4.

The accuracy of the source localization depends on the strength of the GW signal and on the network configuration. With only one detector in the network, the likelihood statistics is constant across the sky (it has no  $\theta$  or  $\phi$  dependence) and therefore the source localization is not possible. However, already with two spatially separated detectors the network becomes sensitive to the source location (see Figure 5). In the case of two closely aligned detectors H1-L1, the area with the large values of the likelihood is rather a ring than a point, showing an ambiguity in the determination of the source location. But even in this case the method gives directional information about the source and allows exclusion of the most of the sky area as inconsistent with the detected GW signal. For two misaligned detectors H1-G1, the source localization is more accurate due to different angular sensitivities of the detectors. Even more accurate estimation of the source coordinates can be obtained with three and more detectors in the network (see Figure 3). The greater the

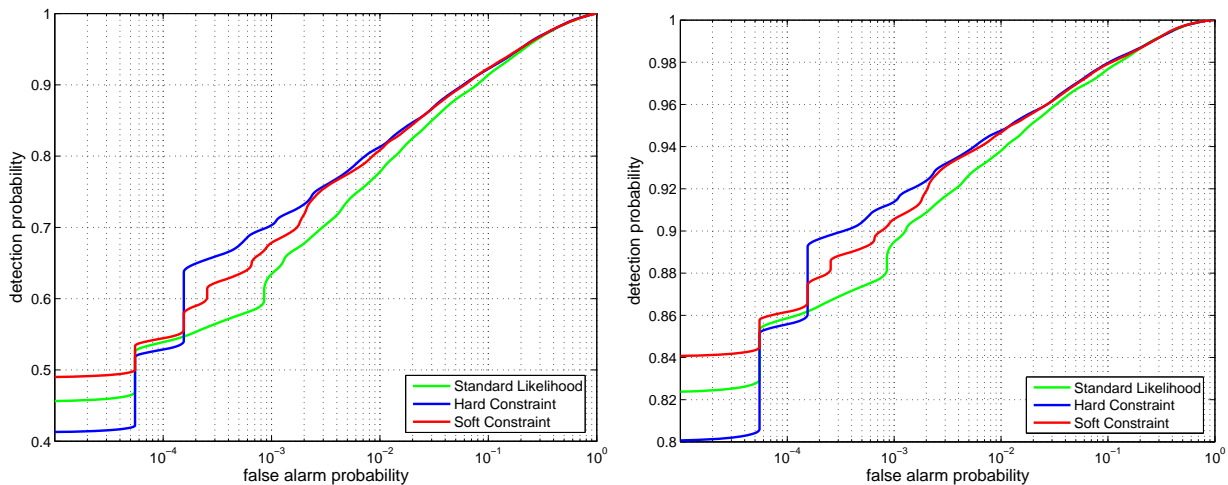


FIG. 4: Receiver operation characteristics for the network of H1-L1-G1 detectors:  $\overline{\text{SNR}} = 6.9$  (left) and  $\overline{\text{SNR}} = 9.2$  (right).

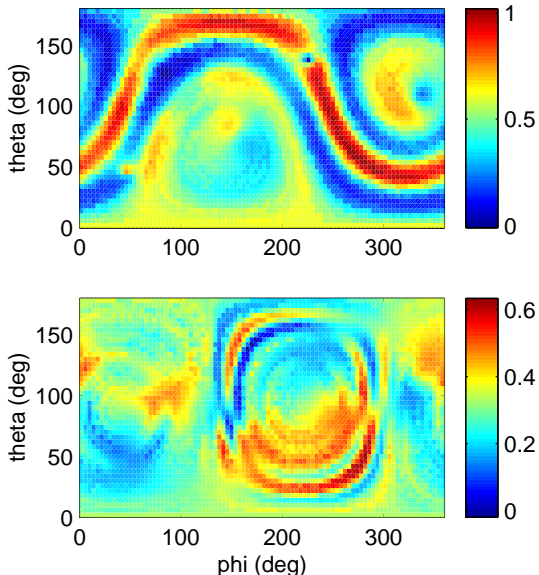


FIG. 5: Sky maps of network statistics for 2 detector networks H1-L1 (top) and H1-G1 (bottom). The source is located at  $\theta = 50^\circ$  and  $\phi = 280^\circ$ .

number of the detectors in the network, the better the source localization.

The error in the source localization is given by the angle  $\alpha$  between the true direction to the source and the reconstructed direction to the source. Equivalently,  $\alpha$  can be defined as the length of an arc connecting these two locations on a sphere with unit radius. To describe the efficiency of the source localization we introduce the following figure of merit. First, we chose a cone with the opening angle  $\alpha_c$  which constitutes an acceptable error. Then we calculate the number of detected sources ( $N_\alpha$ )

which satisfy the condition  $\alpha < \alpha_c$ . The ratio of  $N_\alpha$  to the total number of injections defines the efficiency of the source localization and depends on the signal-to-noise ratio  $\overline{\text{SNR}}$ .

Figure 6 shows the efficiencies of the source localization for the L1-H1-G1 network corresponding to the different detection methods. In this example, the values of the acceptable localization error are chosen to be  $\alpha = 8^\circ$  and  $\alpha = 16^\circ$ . Note that the constraint likelihood methods perform considerably better than the standard likelihood method. Let us consider, for example, the source localization for  $\overline{\text{SNR}}$  of 10 (20). The hard constraint method recovers approximately 48% (66%) of all simulated sources within the 8-degree angle from their true location. In comparison, the standard likelihood method yields only 12% (35%) efficiency for the same angle. Within the 16-degree angle, the hard constraint method recovers 66% (86%) of all the simulated sources, whereas the standard method yields only 22% (50%) efficiency. Similar comparisons hold for the soft constraint method. We find that for both constraint likelihood methods, the events with poorly reconstructed coordinates come from the areas in the sky with small values of the network sensitivity.

## VIII. CONCLUSION

We have presented a novel approach to the detection and reconstruction of gravitational waves with an arbitrary network of interferometric detectors. Starting with the network likelihood ratio functional for unknown gravitational wave burst signals, we identify and solve the two detector paradox. The essence of the paradox is that in the case of two arbitrary misaligned detectors the maximum likelihood ratio statistics depends only on the power in the detector data streams. It does not agree with the statistic of two co-aligned detectors, which de-

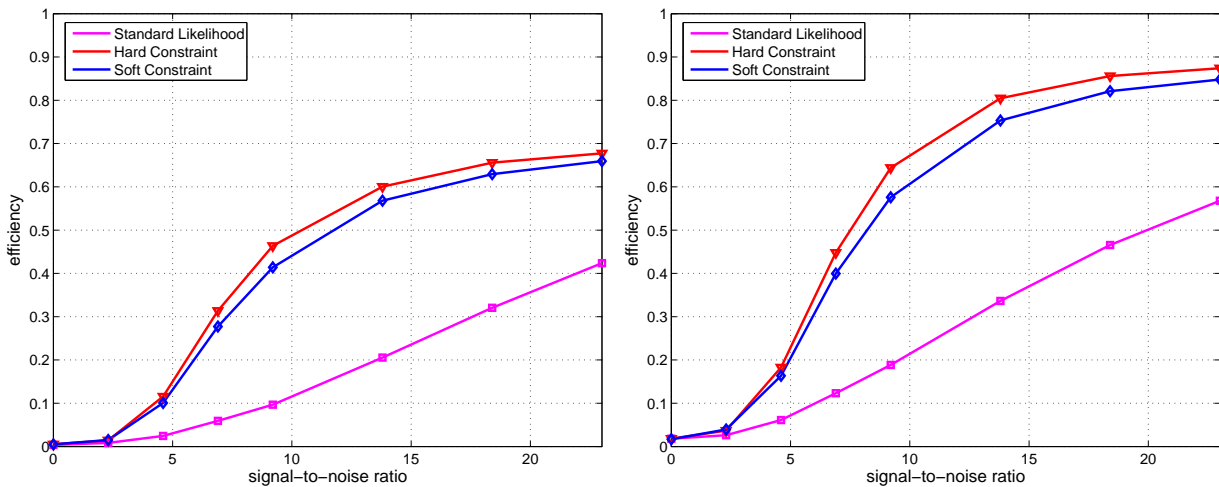


FIG. 6: Efficiency of the source localization with a network of three detectors H1-L1-G1:  $\alpha_c = 8$  (left),  $\alpha_c = 16$  (right).

depends also on the cross-correlation between the detectors. We show that the problem is associated with the different sensitivity of the detector network to two polarization components of the GW signal and present not only in the case of two detectors, but for any arbitrary network. To characterize the difference in the sensitivity to the GW components, we introduce the network alignment factor. For locations on the sky where the value of the alignment factor is small, the network is sensitive to only one GW component and the variation of the likelihood functional results in the un-physical solutions for the second GW component. To exclude the un-physical solutions we propose to use constraints, which limit the parameter space of the GW waveforms and result in a new class of the maximum likelihood ratio statistics. For the networks of two and more detectors, the constraint likelihood methods allow reconstruction of the two GW polarization components and the location of the source on the sky.

In the paper we introduce two examples of the constraint statistics, which performance is compared with the standard likelihood statistics. The performance of the method was estimated with the numerical simulation. We restricted our simulation to the case of the white Gaussian noise. For simplicity we assumed that all

detectors have identical sensitivities though the method presented in this paper does not have these restrictions. Our simulation results indicate that the constraint likelihood method enhance the detection of the GW signals and performs significantly better than the standard likelihood method in the reconstruction of the source coordinates. We believe that since all the methods we have considered are compared on exactly the same footing, our results regarding relative performance will not change for the general case. However, as a work in progress, we plan to expand our simulations to more realistic detector noise.

## IX. ACKNOWLEDGMENTS

We thank Jolien Creighton for usefull discussion and comments on the paper. We also thank Erik Katsavounidis, Peter Saulson, Massimo Tinto and Patrik Sutton for comments on the paper. This work was supported by the US National Science Foundation grants PHY-0244902, PHY-0070854 to the University of Florida, Gainesville and NASA grant NAG5-13396 to the Center for Gravitational Wave Astronomy at the University of Texas at Brownsville.

---

[1] A. Abramovici *et al*, *Science* **256**, 325 (1992).  
 [2] F. Acernese *et al*, *Class. Quantum Grav.* **21**, S385 (2004).  
 [3] B. Willke *et al*, *Class. Quantum Grav.* **21**, S417 (2004).  
 [4] M. Ando and the TAMA collaboration, *Class. Quantum Grav.* **19**, 1409 (2002).  
 [5] International Gravitational Event Collaboration (IGEC), URL: <http://igec.lnl.infn.it/>  
 [6] Kimberly C.B. New, “Gravitational Waves from Gravitational Collapse”, *Living Rev. Relativity*

**6**, (2003), 2. URL (cited on June 16, 2005): <http://www.livingreviews.org/lrr-2003-2>  
 [7] É. Flanagan and S. A. Hughes, *Phys. Rev. D* **57**, 4535 (1998).  
 [8] S. Kobayashi and P. Mészáros, *Astrophys. J.* **589**, 861 (2003).  
 [9] Y. Guersel and M. Tinto, *Phys. Rev. D* **40**, 3884 (1989).  
 [10] É. Flanagan and S. A. Hughes, *Phys. Rev. D* **57**, 4566 (1998).  
 [11] C. W. Helstrom, *Statistical Theory of Signal Detection*,

- 2nd ed. (Pergamon press, London, 1968).
- [12] A. Stuart and K. Ord, *Kendall's Advanced Theory of Statistics*, Vol.2, 5<sup>th</sup> Edition (Edward Arnold, 1991).
  - [13] W. Anderson *et al*, Phys. Rev. D **63**, 042003 (2001).
  - [14] J. Sylvestre, Phys. Rev. D **68**, 102005 (2003).
  - [15] N. Arnaud *et al*, Phys. Rev. D, **68** 102001 (2003).
  - [16] L. S. Finn, Phys. Rev. D **63**, 102001 (2001).
  - [17] L. Cadonati, Class. Quantum Grav. **21**, S1695 (2004).
  - [18] B. Abbott *et al*, Phys. Rev. D **69**, 102001 (2004).
  - [19] M. Rakhmanov and S. Klimentko, Submitted to Proc. of 9<sup>th</sup> *Gravitational Wave Data Analysis Workshop*, Annecy, France (2004).
  - [20] L. Wen and B. F. Schutz, Submitted to Proc. of 9<sup>th</sup> *Gravitational Wave Data Analysis Workshop*, Annecy, France (2004).
  - [21] Wm. R. Johnston, *Detection strategies for a multi-interferometer triggered search*, Master's thesis, The University of Texas at Brownsville (2004).
  - [22] C. Misner, K. Thorne, J. Wheeler, *Gravitation*, Chapter 38 (Freeman, San Francisco, 1973).
  - [23] S. Dhurandhar and M. Tinto, Mon. Not. R. Astr. Soc. **234**, 663 (1988).
  - [24] W. Althouse *et al*, *Determination of Global and Local Coordinate Axes for the LIGO Sites*, LIGO-T980044-08-E (1999).
  - [25] A. Pai, S. Dhurandhar, S. Bose, Phys. Rev. D **64**, 042004 (2001).
  - [26] S. Mohanty *et al*, Class. Quantum Grav. **21**, S1831 (2004).
  - [27] G. Arfken, *Mathematical Methods for Physicists*, Chapter 17, pp. 945-950, 3rd ed. (Academic Press, Orlando, 1985).
  - [28] J. Baker *et al*, Phys. Rev. D **65**, 124012 (2002).
  - [29] This quantity is not the total physical energy carried by the gravitational wave.